

See discussions, stats, and author profiles for this publication at: <https://www.researchgate.net/publication/231639821>

Comprehensive Theoretical Study of the Conversion Reactions of Spiropyrans: Substituent and Solvent Effects

ARTICLE · SEPTEMBER 2004

CITATIONS

25

READS

46

2 AUTHORS, INCLUDING:



Yinghong Sheng

Florida Gulf Coast University

35 PUBLICATIONS 411 CITATIONS

SEE PROFILE

Comprehensive Theoretical Study of the Conversion Reactions of Spiropyrans: Substituent and Solvent Effects

Yinghong Sheng and Jerzy Leszczynski*

The Computational Center for Molecular Structure and Interactions, Department of Chemistry, Jackson State University, P.O. Box 17910, 1400 J. R. Lynch Street, Jackson, Mississippi 39217

Antonio A. Garcia and Rohit Rosario

Harrington Department of Bioengineering, Arizona State University, Tempe, Arizona 85287

Devens Gust and Joseph Springer

Department of Chemistry and Biochemistry, Arizona State University, Tempe, Arizona 85287

Received: March 12, 2004; In Final Form: June 23, 2004

A comprehensive theoretical study of the reaction mechanisms for the conversion between spiropyrans (SPs) and the open form of merocyanines (MCs) has been conducted by theoretical calculations. The reaction mechanisms on the ground- and triplet-state potential energy surfaces (PESs) were investigated using the density functional method. Time-dependent density functional theory (TD-DFT) calculations using the CIS optimized excited-state geometries were carried out to study the reaction mechanisms on the lowest excited singlet-state PES. Two possible reaction mechanisms for the thermal conversion between SPs to MCs were found on the ground-state PES. The geometrical parameter, BLA (Bond Length Alternation), which correlates the strengths of the substituents and the polarities of solvents, was used to explain the changes in the reaction mechanism induced by the different donor–acceptor pairs and solvents. In addition, the reaction mechanisms of spiropyran \rightleftharpoons merocyanine conversion on the triplet and the lowest excited singlet potential energy surfaces were also studied; several possible reaction mechanisms on the excited-state PESs were proposed. A comprehensive mechanistic view of the ultrafast photochemistry of spiropyrans was revealed and interpreted in terms of the strengths of substituents and the polarity of solvents.

I. Introduction

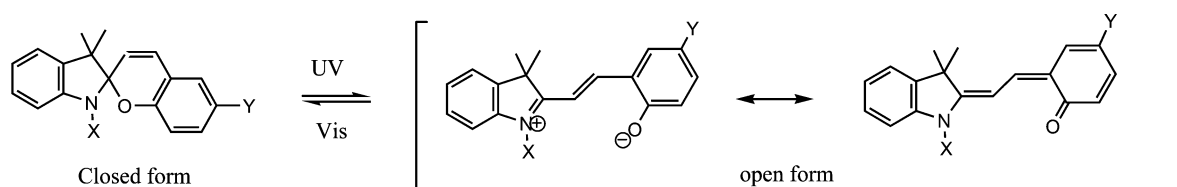
Photochromism via photoisomerization of molecules has been extensively studied for applications such as the modification of the optical properties of materials upon light irradiation and as a component of photogray optical lenses.^{1,2} Recently, there has been a resurgence of interest in photochromism for optical memory and switch applications.³ Of particular interest is a class of molecules known as spiropyrans. Spiropyrans are photochromic materials that have been extensively studied due to their potential applications in several important areas, including high-density optical storage, optical switching, image processing, and display. The photoswitchability of spiropyrans has recently begun to be exploited as a means of reversible light modulation of properties of a variety of chemical assemblies and has been used for photocontrol of enzyme activity,⁴ surface patterning, optical signal transduction, membrane permeability, and surface wetting.⁵

The spiropyrans comprise a group of light-switchable, photochromic organic molecules. Among various kinds of spiropyrans, 1'-3'-3'-trimethyl-6-nitrospiro[2H-1-benzopyran-2,2'-indoline] (6-nitro-BIPS) has been intensively studied.⁶ The majority of spiropyrans exist in the dark as a nonpolar closed form that absorbs light only in the ultraviolet region. When exposed to UV light, the spiropyran undergoes a molecular rearrangement that produces an open form. The open form of spiropyrans (also called *trans*-merocyanine (MC)) is colored.

The open form of spiropyrans can revert back to the closed form thermally or photochemically. Thus, the molecules may be switched from the closed to the open form (coloration) with UV light (or thermally in the dark in polar solvents), and from the open form to the closed form (decoloration) with visible light, or thermally with typical time scales of microseconds⁷ (see Scheme 1). The photochromism of the spiropyran/*trans*-merocyanine pair has been reviewed previously.⁸ The rate and mechanism of the reaction of some spiropyrans and their analogues have been examined with continuous absorption spectroscopy,⁹ transient absorption spectroscopy, and transient Raman spectroscopy.¹⁰

Due to the complex nature of the reaction, several mechanisms have been proposed. The homolytic process has been considered, and indirect evidence of a biradical transient formation has been provided by spin-trapping experiments.¹¹ Because of its extremely low concentration, the biradical is most likely not to appear on the main reaction pathway that originates photochromism. Several authors have proposed that the light-induced opening of the pyran ring is essentially a heterolytic process, yielding a short-lived transient species that rearranges in less than 100 ps to give the merocyanine(s). Investigations by transient nanosecond and picosecond spectroscopy and laser flash photolysis, as well as ligand/metal-ion complexation of bidentate MCs that traps the *cis*-MC form,^{12,13} have led to the observation of the high-energy *cis*-form as a transient intermediate.^{14,15} Malatesta et al.¹⁶ also succeeded in isolating spiro-

SCHEME 1



oxazine (SO) and zwitterion derivatives (ZWA) formed by chemical trapping of the MC zwitterions of SOs with trimethylsilyl cyanide (TMSCN), supporting the strong polarization of the MC ground state. Therefore, the conversion between the closed-form spiropyran (SP) and the open-form spiropyran (MC) that has been proposed should have at least two steps, with *cis*-MC being the intermediate on the reaction potential surface.

Several species have been detected from transient absorption spectroscopy when the spiropyrans were exposed to UV light. One long-lived species has been assigned as the *trans*-merocyanine. The short-lived species, according to their characteristics, have been assigned as the triplet states of *trans*-merocyanine or *cis*-merocyanine.¹¹ This raises the question of SP-MC conversion and, in particular, of the role of the triplet states in the photochemical reaction. Some studies propose the triplet pathway¹⁷ while others support the singlet pathway.¹⁸ Though this has been the subject of many studies, there is still no agreement as to whether the reaction proceeds through the singlet or the triplet state.

Most theoretical studies have been conducted on simple model compounds. Day et al.¹⁹ investigated the ground-state ring opening of pyran, a model compound of spiropyran, to mimic the thermal ring opening of spiropyran. The ring opening of pyran was reported to be a two step reaction. The second step, *cis*–*trans* isomerization, has a negligible barrier. However, the ring-opening reaction mechanism for spiropyran has not been discussed. Only the relative energies of open merocyanine with respect to the closed spiropyran and nitrochromene were reported. The reaction mechanism of the SP-MC conversion, however, is different from pyran. The thermochromism of 1,3,3-trimethylspiro[indoline-2,3'-naphtho[2,1-b]-[1,4]oxazine] (SO), an analogue of spiropyran, has also been studied using the DFT method.²⁰ An extensive description of the ground-state ring opening/closing and isomerization process of eight open forms was proposed. The reaction mechanism of the thermal conversion of SO is expected to be similar to that of spiropyran.

Fewer theoretical studies of the excited-state species have been reported due to the difficulties in the prediction of the excited-state properties. Among such studies, most applied semiempirical methods coupled with the single-excitation configuration interaction based on the ground-state equilibrium geometries or along reaction coordinates obtained through constrained optimizations.²¹ Robb et al. have studied the excited singlet potential surface and the ground-state potential surface for the cleavage of the C–O bond in the benzopyran at the CASSCF level.²² They have demonstrated a conical intersection between the S_1 and S_0 state potential surfaces, indicating a great potential that the excited-state system can undergo efficient decay to the ground state at the crossing point. However, only the C–O cleavage step on the excited singlet-state PES has been studied, while the information for the triplet state is still unavailable.

Despite these efforts, the detailed dynamics of spiropyran compounds have not been clarified, and unsolved problems concerning the spiropyran \rightleftharpoons merocyanine (SP \rightleftharpoons MC) transforma-

tion remain. For instance, the intimate structure of the photochemically produced colored species, the nature of any reaction intermediates, and the detailed mechanistic processes involved in the thermally and photochemically reversible pathways between SP and MC are still unclear. The experimental and theoretical studies available so far provide only a fragmentary mechanistic picture of the photochromism/thermochromism process. Comprehensive knowledge of the SP \rightleftharpoons MC conversion mechanisms on the ground state and the lowest excited-state PESs are needed. This is of importance for the rational design of new photochromic compounds with improved performance. Therefore, in this paper the results of detailed investigations of the possible reaction mechanisms for the conversion between spiropyrans and merocyanines on the ground state and the lowest excited-state potential surfaces are reported. In addition, the substituent and solvent effects are also discussed. The data computed for three electronic states (S_1 , T_1 , S_0) provide a comprehensive mechanistic view of the ultrafast photochemistry of the spiropyrans.

II. Calculation Method and the Model Compounds

Ground-State and Triplet-State Calculations. The choice of theoretical level depends on the accuracy requested and the size of a molecule. Correlation energy correction is necessary for a reasonable prediction of the activation energy because the contribution of the correlation energy is often larger for the transition structures than for the minimum energy structures. The DFT-B3LYP method has been demonstrated to predict excellent geometries and energies.²³ In addition, this level of computation was found to take into account both localized structures, quinoidal and zwitterionic, for merocyanine isomers. Therefore, the conversion between spiropyrans and merocyanines for the ground- and triplet-state species was studied using the B3LYP nonlocal density functional approximation.²⁴ The geometry of the reactants, products, transition states, and intermediates were optimized by means of the Berny approach, a modified Schlegel method.²⁵ Vibration frequency calculations were performed to confirm whether the obtained geometry represents a transition or minimum energy structure.

The reaction mechanism was also studied in the solvents. The useful form to describe nonspecific solute–solvent interaction is provided by the polarized continuum model using the integral equation formalism.²⁶ In this model, the liquid is represented by a dielectric continuum, characterized by its dielectric constant ϵ . The solute is placed in a cavity created in the continuum. The distribution of electronic density of the solute polarizes the continuum and generates an electric field inside the cavity, which in turn affects the geometry and electronic structure.

To qualitatively assess the solvent effect for a significant range of solvents, the dielectric constants of $\epsilon = 20.7$ and $\epsilon = 78.39$ (corresponding to acetone and water, respectively), were used. The geometry of the reactants, products, transition states, and intermediates were reoptimized in the solvents. The specific interactions, such as hydrogen bonding, are not included in this model.

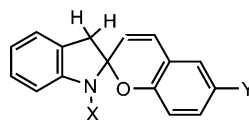
The 6-31G(d) basis set has been proven to reproduce well the geometrical parameters. The further expansion of the basis set has less impact on the accuracy of the molecular parameters.²⁷ Broo and Holmén²⁸ also reported that only minor changes of the geometrical parameters for spiropyrans were observed when the basis set was extended in their B3LYP calculations. The 6-31G(d) basis set is a good compromise between efficiency and accuracy.²⁸ We have also used the 6-311+G(d) basis set for some of the studied species and obtained similar results. Therefore, we will report the results obtained from the 6-31G(d) basis set unless otherwise mentioned.

Excited Singlet-State Calculations. Despite progress in this field, it is still quite difficult to calculate the properties of molecules in their electronic excited states, especially for relatively large molecular systems.²⁹ Compared to the ground-state studies, few calculations have been published for the excited states, and even fewer considered changes in molecular structure upon excitation. However, many photochemical processes require excited-state geometry optimizations as significant conformational relaxations take place after photoexcitation.

Much effort has been put into the development of methods for the optimization of the excited state, but so far only a few efficient techniques are available, even for small organic systems. The complete active space self-consistent field (CASSCF)³⁰ method represents an approach that allows for geometry optimization of the electronic excited states. However, only a relatively few orbitals can be included in the complete molecular orbital active space. The computational cost is also a serious problem when dealing with large systems. There has been significant progress in the development of DFT-based methods for the excited-state properties, namely the time-dependent density functional theory (TD-DFT)^{31,32} and a combination of DFT with the single and multireference configuration interactions (DFT/SCI and DFT/MRCI). Recently, excited-state gradients have also been implemented in DFT.³³ However, further investigation is required before the quantitative accuracy can be assessed. The single-reference configuration interaction with the single excitation (CIS) method³⁴ has been also frequently used. It allows the optimization of the excited-state geometry of relatively large molecules; therefore, the CIS method may still be the desirable way to study systematically the lowest excited state for a series of spiropyrans with different substituents. It is well known that the CIS excitation energies are always higher than the experimental values, while the TD-DFT excitation energies have been proved to be in close agreement with the experimental values.³⁵ Therefore, TD-DFT single-point calculations using the excited-state geometries obtained from the CIS optimizations were carried out in this work. By doing so, one can compare the relative energies with the ground and triplet states and better understand the entire picture of the photochromic reactions for spiropyrans. All calculations were carried out using the Gaussian98 program.³⁶

Model Compounds. One of the best known spiropyrans is 1'-3'-3'-trimethyl-6-nitrospiro[2H-1-benzopyran-2,2'-indoline] (6-nitro-BIPS). To study the substituent effect, a series of combinations of electron-donating and electron-withdrawing groups (**SP-1** – **SP-5**) were investigated, as shown in Scheme 2. Two donor–acceptor substituted patterns were investigated: spiropyran **SP-2** is a weak donor–acceptor substituted spiropyran; **SP-3** stands for a stronger donor–acceptor ($X = \text{Me}$, $Y = \text{NO}_2$) substituted spiropyran. For comparison, an unsubstituted (**SP-1**, $X = Y = \text{H}$), an acceptor–donor (**SP-4**,

SCHEME 2



Closed form

- SP-1.** $X = \text{H}$, $Y = \text{H}$
SP-2. $X = \text{H}$, $Y = \text{NO}_2$
SP-3. $X = \text{Me}$, $Y = \text{NO}_2$
SP-4. $X = \text{H}$, $Y = \text{OMe}$
SP-5. $X = \text{NO}_2$, $Y = \text{NO}_2$

$X = \text{MeO}$, $Y = \text{H}$), and an acceptor–acceptor substituted spiropyran (**SP-5**, $X = Y = \text{NO}_2$) were also considered.

III. Results and Discussion

III-A. Thermal Coloration and Decoloration of Spiropyrans.

Thermal Coloration. Using **SP-2** as the model compound, two alternative pathways (pathway A and pathway B, see Figure 1) of the coloration on the ground-state potential surface have been investigated. On pathway A, the cleavage of the C–O bond in the closed spiropyran takes place, in which the O atom of the benzopyran part is closer to the $-\text{CH}_2-$ group of the dihydroindole moiety. The C–O bond can also be broken in the opposite direction, in which the O atom is closer to the NH group of the dihydroindole moiety (pathway B). The optimized XYZ coordinates and calculated total energies of the closed-form and open-form spiropyran, transition states, and the intermediates involved in the conversion reaction between the closed- and open-form spiropyrans are given in Table S1 of the Supporting Information. The optimized structures are illustrated in Figure 1 along with the relative energies with respect to that of the closed-form spiropyran (**SP**).

As one can see from Figure 1, the closed-form spiropyrans consists of a pyran fragment and another benzopyran moiety that are held almost orthogonally by a chiral “spiro” carbon atom. The $\text{C}_1\text{—O}$ bond length in the closed-form spiropyran (**SP**) is calculated to be about 1.475 Å. The $\text{C}_2\text{—C}_3$ bond of 1.340 Å has double bond character.

A transition state species (**TS1**) on pathway A was located. The $\text{C}_1\text{—O}$ distance elongates to 2.358 Å, indicating that the $\text{C}_1\text{—O}$ bond is significantly broken. The O atom of the phenol part is closer to the $-\text{CH}_2-$ group of the dihydroindole moiety with the dihedral angle $\text{C}_1\text{—C}_2\text{—C}_3\text{—C}_4$ being about 21.31°. The B3LYP/6-31G(d) level activation energy for the C–O bond cleavage is 17.41 kcal/mol.

A *cis*-merocyanine intermediate (**TCC**) is formed via the C–O cleavage transition states (**TS1**). T and C denote *trans* and *cis* forms, respectively, for the dihedral angles $\text{N—C}_1\text{—C}_2\text{—C}_3$, $\text{C}_1\text{—C}_2\text{—C}_3\text{—C}_4$, and $\text{C}_2\text{—C}_3\text{—C}_4\text{—C}_7$. The dihedral angle $\text{C}_1\text{—C}_2\text{—C}_3\text{—C}_4$ (23.2°) remains almost the same as that in the transition state. The distance between the C_1 and O atoms further increases to 3.067 Å in **TCC**. Notably, there is strong H bonding in the **TCC**; the O–H distance amounts to 1.832 Å.

The **TCC** intermediate undergoes *cis*–*trans* isomerization to an open merocyanine. Even the $\text{C}_2\text{—C}_3$ bond (1.397 Å) in **TCC** develops more significant single bond characteristics compared to that in the closed-form spiropyran. It is still not a typical single bond; therefore, a high rotation barrier around the $\text{C}_2\text{—C}_3$ bond (18.75 kcal/mol) is predicted. The corresponding transition state (**TS2**) is shown in Figure 1. The phenol moiety is almost perpendicular to the dihydroindole ring, with the dihedral angle $\text{C}_1\text{—C}_2\text{—C}_3\text{—C}_4$ being about 90°. In *trans*-merocyanine (**TTC**), the two isolated π -conjugated systems, which are noninteracting in the closed form, are extensively conjugated.

Pathway B is similar to pathway A. The C–O bond cleavage transition state (**TS3**) on pathway B was located and is shown

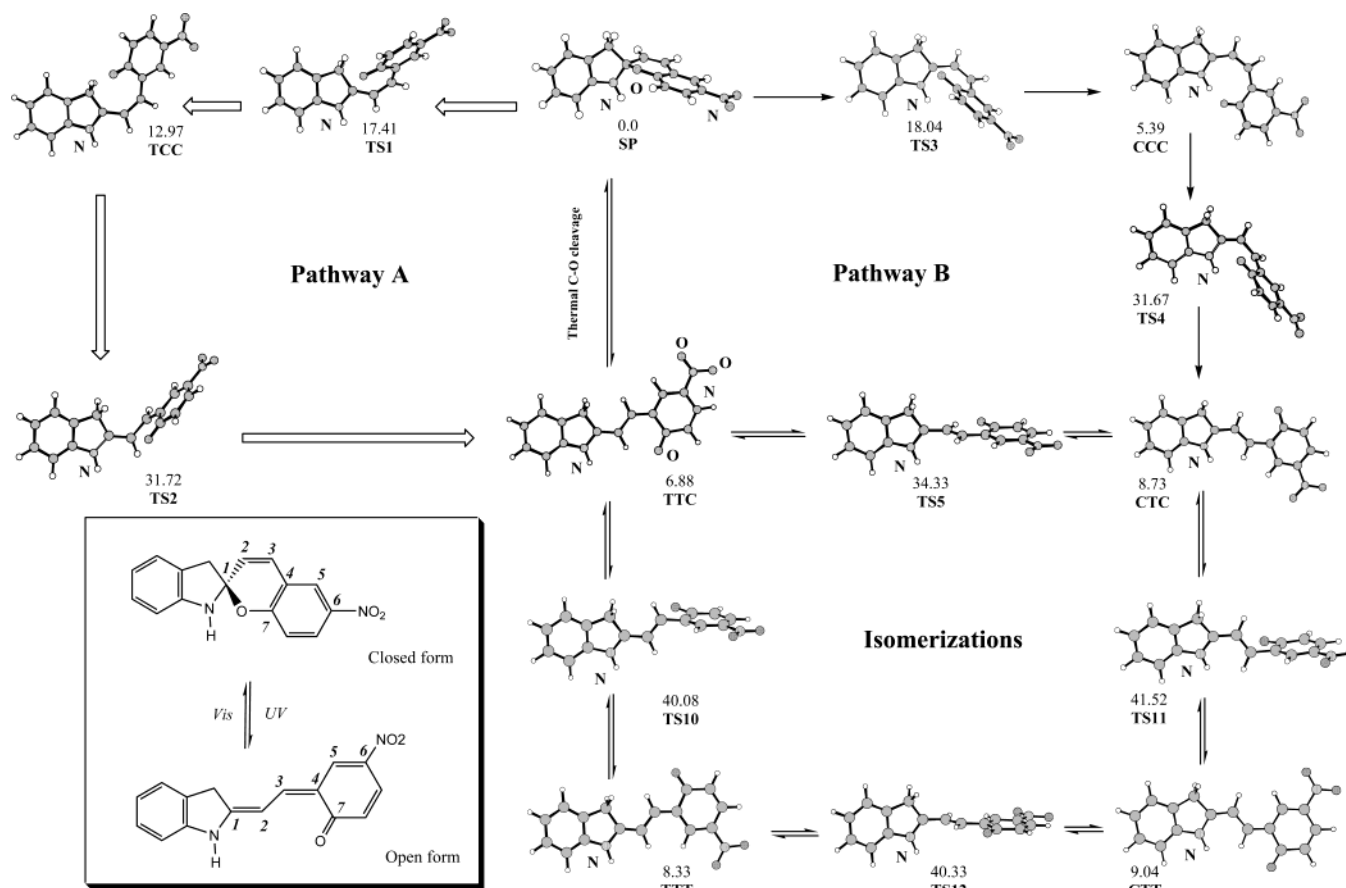


Figure 1. B3LYP/6-31G(d) optimized spiropyran, merocyanins, transition states, and intermediates on reaction pathways A and B of inversion between spiropyran and merocyanine. The relative energies with regard to the closed-form spiropyran are also listed (in kcal/mol).

in Figure 1. The O atom is at the N-side with the dihedral angle $C_1-C_2-C_3-C_4$ being -20.7° . The C_1-O bond distance amounts to 2.326 Å. The calculated activation energy (18.04 kcal/mol) is 0.63 kcal/mol higher than that of **TS1** on pathway A. After C–O cleavage, another *cis*-merocyanine (**CCC**) is located. It is characterized by a small dihedral angle $C_1-C_2-C_3-C_4$ in **CCC** (-9.5°). The O atom is closer to the hydrogen atom of the NH group. Compared to the **TCC** intermediate, **CCC** is more stable (by 7.58 kcal/mol). The higher stability of *cis*-intermediate **CCC** is due to its shorter $O\cdots H$ distance (1.502 Å). The *cis*-merocyanine (**CCC**) isomerizes to *trans*-merocyanine (**CTC**) via the transition state **TS4** with the activation energy of the *cis*–*trans* isomerization being 26.28 kcal/mol.

In brief, both pathways A and B represent two-step reactions: the first step is the cleavage of C–O bond and the second step is the isomerization from *cis*- to *trans*-merocyanine. The second step is the rate-determining step for **SP-2**. Comparing these two pathways, one can conclude that pathway A is favored over pathway B by 7.53 kcal/mol.

Thermal Decoloration. According to the potential energy surfaces shown in Figure 2, pathway B of the thermal decoloration from *trans*-merocyanine to **SP** is favored over pathway A by 1.9 kcal/mol. Both pathways of the decoloration represent two-step reactions: at first the *trans*-merocyanine (**TTC/CTC**) isomerizes to *cis*-merocyanine (**TCC/CCC**) via *trans*–*cis* isomerization, and the second step is the ring closure that leads to the C–O bond formation. The *trans*–*cis* isomerization is the rate-determining step, and the activation barriers are calculated to be 24.84 and 22.94 kcal/mol, for pathways A and B, respectively.

III-B. Thermal Isomerization between Four *trans*-Merocyanines. Four open merocyanine conformers with the central

transoid segment are expected for spiropyran **SP-2** after the thermal or photochemical cleavage of the C–O bond. The four conformations of the open form of spiropyran are labeled as **CTC**, **CTT**, **TTT**, and **TTC** (Figure 1). A crystallographic study indicates that the most stable structure for the open merocyanines in the crystalline phases is the most thermodynamically stable **TTC** isomer.³⁷ Our results are in a good agreement with the experiments.

The relative energies of the four isomerization transition states are shown in Figure 2. One can see that the activation energies for the isomerization between two *trans*-merocyanines are larger than 25 kcal/mol. This indicates that there is a smaller chance for transformation among these four isomers on the ground-state PES. The calculated activation energies are slightly larger than the experimental values (~ 19 kcal/mol) derived from 1H NMR line shape analysis at various temperatures.³⁸

Both pathways A and B could be responsible for the coloration and decoloration processes. The previous experimental study³⁹ on spirooxazine indicated that C–O cleavage resulted in the formation of mainly **TTC** and **CTC** merocyanine isomers. The amount of **CTC** is smaller than that of **TTC**. A recent combined experimental and theoretical study⁴⁰ also demonstrated that **TTC** was mainly present as open merocyanine after the isolated closed-form 1',3'-dihydro-1',3',3'-trimethyl-6-nitrospiro[2-H-1-benzopyran-2,2'-[2H]indole] in a low temperature argon matrix was exposed to UV light.

One should notice that the model compound considered in this work does not possess two methyl groups on the tetrahedral carbon of indoline. The strong steric repulsion induced by these two methyl groups may hinder the pathway A C–O cleavage. Thus, pathway B could be the favorable ring-opening pathway.^{20,41} Our results show that the ring opening of **SP** proceeds

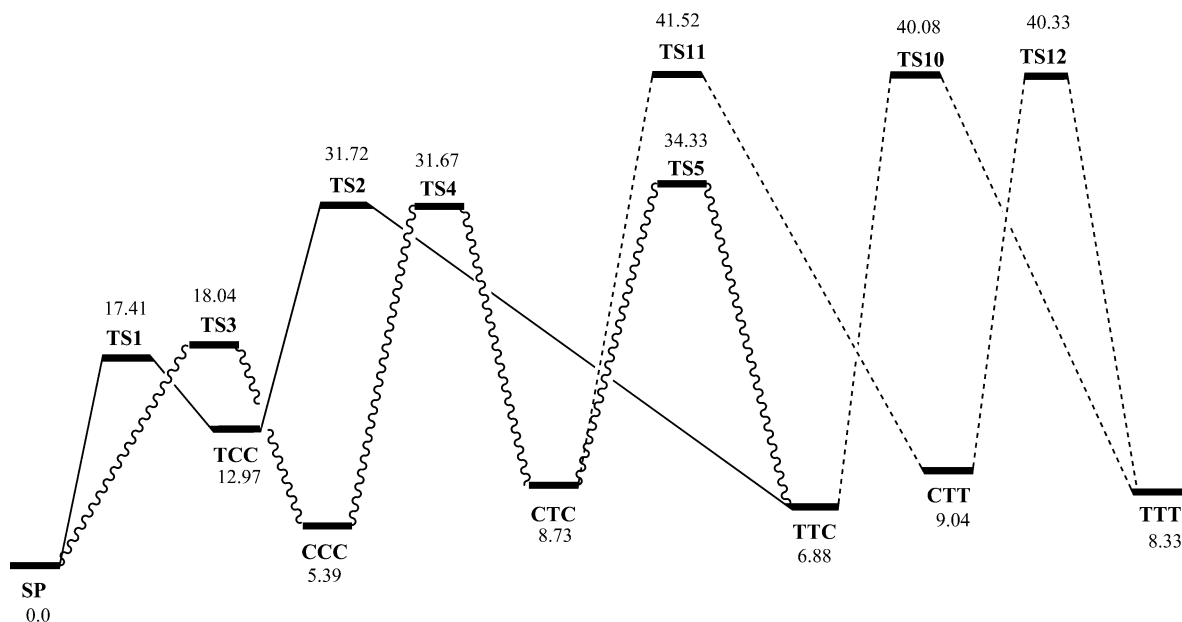


Figure 2. Ground-state potential surfaces for the conversion between spiropyran and merocyanine (pathway A, solid lines and pathway B, wavy lines) and the isomerization between four *trans*-merocyanines, CTC, TTC, CCT, and TTT (dash lines).

TABLE 1: B3LYP/6-31G(d) Calculated Activation Energies for Ring Opening Step and the *cis*–*trans* Isomerization as well as C_1 –O in the Closed-Form SP; the C_2 – C_3 Bond Length in *cis*- and *trans*-MC; and the BLA Values of *trans*-MCs

code	X	Y	SP → MC coloration		MC → SP decoloration		C_1 –O in SP	C_2 – C_3 in <i>cis</i> -MC	C_2 – C_3 in <i>trans</i> -MC	BLA in <i>trans</i> -MC
			$\Delta E^\ddagger_{\text{ring opening}}$	$\Delta E^\ddagger_{\text{cis-trans}}$	$\Delta E^\ddagger_{\text{trans-cis}}$	$\Delta E^\ddagger_{\text{ring closure}}$				
SP-1	H	H	21.61	14.77	20.45	6.23	1.4598	1.4070	1.4114	0.033
SP-2	H	NO ₂	17.41	18.75	24.84	4.44	1.4751	1.3974	1.4016	0.013
SP-3	Me	NO ₂	15.44	18.57	25.10	3.32	1.4816	1.3975	1.4010	0.011
SP-4	H	MeO	21.81	13.08	18.93	7.35	1.4561	1.4104	1.4128	0.037
SP-5	NO ₂	NO ₂	28.43	9.11	13.87	5.73	1.4363	1.4188	1.4214	0.043

more readily via pathway A than via pathway B. Therefore, only characteristics of pathway A have been further investigated.

III-C. Substituent Effect. It is well known that 1',3',3'-trimethylspiro[2H-1-benzopyran-2,2'-indoline] (BIPS) can be transformed photochemically into merocyanine, which isomerizes thermally with a very high reverse rate for decoloration.⁴² Therefore, unsubstituted BIPS has no practical value with respect to photochromism. On the other hand, a nitro group in the 6-position of the benzopyran part (for instance, 6-NO₂–BIPS) enhances photochromic activity.⁴³ Nitro group substitution leads also to higher degradation process. Therefore, the substituents play an important role in the photochemistry of spiropyran. To study the substituent effect on the reaction mechanism, we used different combinations of electron-donating and electron-withdrawing groups⁴⁴ on either the X or Y position. The five substituted spiropyran, SP-1 to SP-5, under investigation are shown in Scheme 2.

The introduction of different donor and/or acceptor groups for a π -conjugated spiropyran leads to various changes in the molecular structures. According to the classic valence bond theory,⁴⁵ the ground state of the open-form merocyanine can be regarded as a resonance hybrid of a zwitterionic structure and a neutral structure, where the degree of mixing of the two structures determines the BLA (Bond Length Alternation) values,⁴⁶ that is, the difference between the average lengths of the single and double bonds in the π -conjugated spiropyran. For donor–acceptor spiropyran, BLA equals $(R_{N-C1} + R_{C2-C3} + R_{C4-C5})/3 - (R_{C1-C2} + R_{C3-C4} + R_{C5-C6})/3$. The definition was chosen so that the spiropyran can be tuned from the neutral resonance form (BLA = +0.1 Å) to the zwitterionic form (BLA = –0.1 Å) with the increasing strength of the donor–acceptor

pairs or the polarity of the solvents. The DFT-calculated BLA values for the selected five substituted spiropyran are listed in Table 1. For unsubstituted spiropyran (SP-1), the DFT-calculated BLA value amounts to 0.033 Å. When an electron-withdrawing group (NO₂) was introduced on the Y position, the BLA decreased to 0.013 Å, indicating a higher contribution from the zwitterionic resonance structure. An even stronger donor–acceptor substituted spiropyran possess a smaller BLA value (BLA = 0.011 Å). To the contrary, introducing an electron-donating group at the Y position or an electron-withdrawing group at the X position will increase the values of the BLA, and the spiropyran will have higher contribution from the neutral resonance structure.

The calculated activation energies for coloration and decoloration are listed in Table 1. For unsubstituted spiropyran (SP-1, X = Y = H), the activation energies for the C–O bond cleavage and the *cis*–*trans* isomerization are 21.61 and 14.77 kcal/mol, respectively. However, for donor–acceptor substituted spiropyran (SP-2, SP-3), the activation energies for the C–O bond cleavage become smaller, while the *cis*–*trans* isomerization activation barriers increase and become the rate-determining step. On the contrary, acceptor–donor and acceptor–acceptor substitutions (SP-4 and SP-5) increase the C–O bond cleavage activation energies and make the C–O cleavage the rate-determining step.

The changes in the activation energies for coloration of five spiropyran species can be interpreted in terms of their C_1 –O and C_2 – C_3 bond lengths as well as their BLA values. As one can see from Table 1, donor–acceptor pairs elongate the C_1 –O bond lengths in the closed-form spiropyran and somewhat decrease the C_1 –O bond strengths, consequently leading to a

TABLE 2: B3LYP/6-31G(d) Calculated Activation Energies for the Ring Opening Step and the *cis*–*trans* Isomerization as well as C₁–O in the Closed-Form SP-2; the C₂–C₃ Bond Length in *cis*- and *trans*-MC; and BLA Values of *trans*-MCs

	SP → MC coloration		MC → SP decoloration		C ₁ –O in SP	C ₂ –C ₃ in <i>cis</i> -MC	C ₂ –C ₃ in <i>trans</i> -MC	BLA in <i>trans</i> -MC
	$\Delta E^{\ddagger}_{\text{ring opening}}$	$\Delta E^{\ddagger}_{\text{cis} \rightarrow \text{trans}}$	$\Delta E^{\ddagger}_{\text{trans} \rightarrow \text{cis}}$	$\Delta E^{\ddagger}_{\text{ring-closure}}$				
gas	17.41	18.75	24.84	4.44	1.475	1.397	1.402	0.013
acetone	12.18	22.17	29.99	3.71	1.482	1.385	1.384	–0.015
water	9.51	24.02	33.37	3.31	1.484	1.380	1.380	–0.030

lower C–O cleavage activation energy. However, donor–acceptor pairs shorten the C₂–C₃ bond lengths in the *cis*-intermediates and therefore result in higher *cis*–*trans* isomerization activation energies.

There is a simple relationship between the BLA value and the activation barriers of the C–O cleavage and the *cis*–*trans* isomerization steps. For spiropyrans with small BLA values (**SP-2**, **SP-3**), the *cis*–*trans* isomerization is the rate-determining step. However, for spiropyrans with large BLA values (**SP-1**, **SP-4**, **SP-5**), C–O cleavage is the rate-determining step. So, the rate-determining step of coloration can be changed using different donor–acceptor pairs. The experimental activation energies for coloration are 24.21, 24.59, and 24.23 kcal/mol for 1'-methyl-spiro[2H-1-benzopyran-2,2'-indoline], 1'-methyl-6-nitrospiro[2H-1-benzopyran-2,2'-indoline], and 1'-methyl-6,8-dinitrospiro[2H-1-benzopyran-2,2'-indoline], respectively.^{47,48–51} No simple correlation between the strength of the donor–acceptor pairs and the coloration activation energies was observed in the experiments. The reason might be that there is a turning point where the rate-determining step changes for different substituted spiropyrans.

The decoloration of spiropyrans at the ground state is relatively simpler. The *trans*–*cis* isomerization is always the rate-determining step, regardless of what kind of substituent is used. From Table 1, one can conclude that there is a monotonic relationship between the *trans*–*cis* isomerization barrier and the BLA values in *trans*-merocyanine. Introducing an acceptor group at X and a donor group at Y positions decreases the BLA value, facilitating the *trans*–*cis* isomerization. Our results are consistent with the experimental data that show that decoloration barriers for the aforementioned spiropyrans monotonically increase from 18.30 to 22.01 and 26.25 kcal/mol as the strengths of donor–acceptor pairs increased.

III-D. Solvent Effect. The solvent effect on the reaction mechanism of the model compound (**SP-2**) was also investigated with relative permittivities of $\epsilon = 20.7$ (acetone) and $\epsilon = 78.39$ (water). The calculated activation energies for coloration and decoloration of **SP-2** are listed in Table 2. The optimized C₁–O bond lengths in the closed-form spiropyran **SP-2**, the C₂–C₃ bond lengths in *cis*- and *trans*-merocyanine, and the BLA values are listed in Table 2.

Similarly to the substituent effect, the relative contribution of the two resonance structures is also affected by the solvents and leads to changes in the BLA values. The solvent effect is similar to the substituent effect described in the preceding section. The BLA value of spiropyran decreases when the polarity of the solvent increases. The number of BLA changes induced by the solvents is much more significant than those of the substituents, and the BLA values even become negative in polar solvents.

Compared to the gas phase, the C₁–O bond length in the closed-form spiropyran elongates as the polarity of the solvent increases, while the C₂–C₃ bond lengths in *cis*-form MC and *trans*-form MC become shorter. Therefore, the C–O cleavage activation energy decreases from 17.41 kcal/mol in the gas phase to 9.41 kcal/mol in the water solution, while the *cis*–*trans*

isomerization activation energies increase from 18.75 to 22.17 and 24.02 kcal/mol in acetone and water, respectively. Therefore, the activation energies for the coloration of spiropyrans increase as the polarities of solvents increase. This is in agreement with the experiment that shows that the activation energies for thermal coloration for 1'-3'-3'-trimethyl-6-nitrospiro[2H-1-benzopyran-2,2'-indoline] (6-nitro-BIPS) increase from 19.4 kcal/mol in benzene to 24.1 and 26.8 kcal/mol in propanol and ethanol, respectively.^{48,49,50} Such a trend is also observed for 1',3',3'-trimethylspiro[2H-1-benzopyran-2,2'-indoline] (BIPS) in different solvents.⁵¹

The *trans*–*cis* isomerization is the rate-determining step for the thermal decoloration of **SP-2**. The ring closure only needs to overcome a comparatively smaller activation energy to form the C–O bond. The decoloration activation energy increases from 24.84 kcal/mol in the gas phase to 29.99 and 33.37 kcal/mol in acetone and water, respectively. Our results reproduce well the experimental trends, although the experimental decoloration activation energies for 6-nitro-BIPS are slightly smaller, being 16.51, 22.01, and 24.64 kcal/mol when the solvent changes from benzene to the more polar propanol and ethanol solvents.

Comparing Table 1 and Table 2, one can find a clear correlation between the activation energies and the BLA values. Decoloration activation energies increase as the BLA becomes smaller. In other words, the decoloration activation energies increase as the strength of the donor–acceptor pairs (or the polarity of solvents) increase. The variation in coloration is slightly more complicated as the coloration activation energy decreases in the BLA = 0.04–0.00 Å range and then increases when the BLA is smaller than 0.00 Å.

We also notice that the coloration activation energy does not increase as much as that for decoloration when the polarities of the solvents or the strengths of the substituents increase. As can be seen in Tables 1 and 2, the activation energy of the coloration and decoloration for **SP-2** (X = H, Y = NO₂) in the gas phase are 18.75 and 24.84 kcal/mol, respectively. The difference is about 6.1 kcal/mol, while the difference increases to 7.8 kcal/mol in acetone and 9.4 kcal/mol in water. Similarly, the $\Delta E^{\ddagger}_{\text{decoloration}} - \Delta E^{\ddagger}_{\text{coloration}}$ difference also increases from 1.1 kcal/mol for **SP-2** (X = H, Y = NO₂) to 6.5 kcal/mol for the stronger donor–acceptor substituted spiropyran, **SP-3** (X = Me, Y = NO₂). Therefore, one can conclude that the polar solvents or stronger donor–acceptor substituents favor the thermal coloration over decoloration. This is consistent with the experimental results that show that the additional nitro group in the 8-position of the benzopyran part leads to a very small amount of the spiro compound appearing in the thermal equilibrium in dipolar solvents.⁵²

III-E. Conversion between Spiropyrans and Merocyanines on the Triplet Potential Surface. In an experiment, ultraviolet light of 340 nm wavelength (~85 kcal/mol) was used to initiate the coloration of spiropyrans. The TD-DFT calculated vertical excitation energy for the closed-form spiropyran **SP-2** is about 73 kcal/mol. Therefore, the closed-form spiropyrans may be promoted to the excited singlet state, followed by radiationless

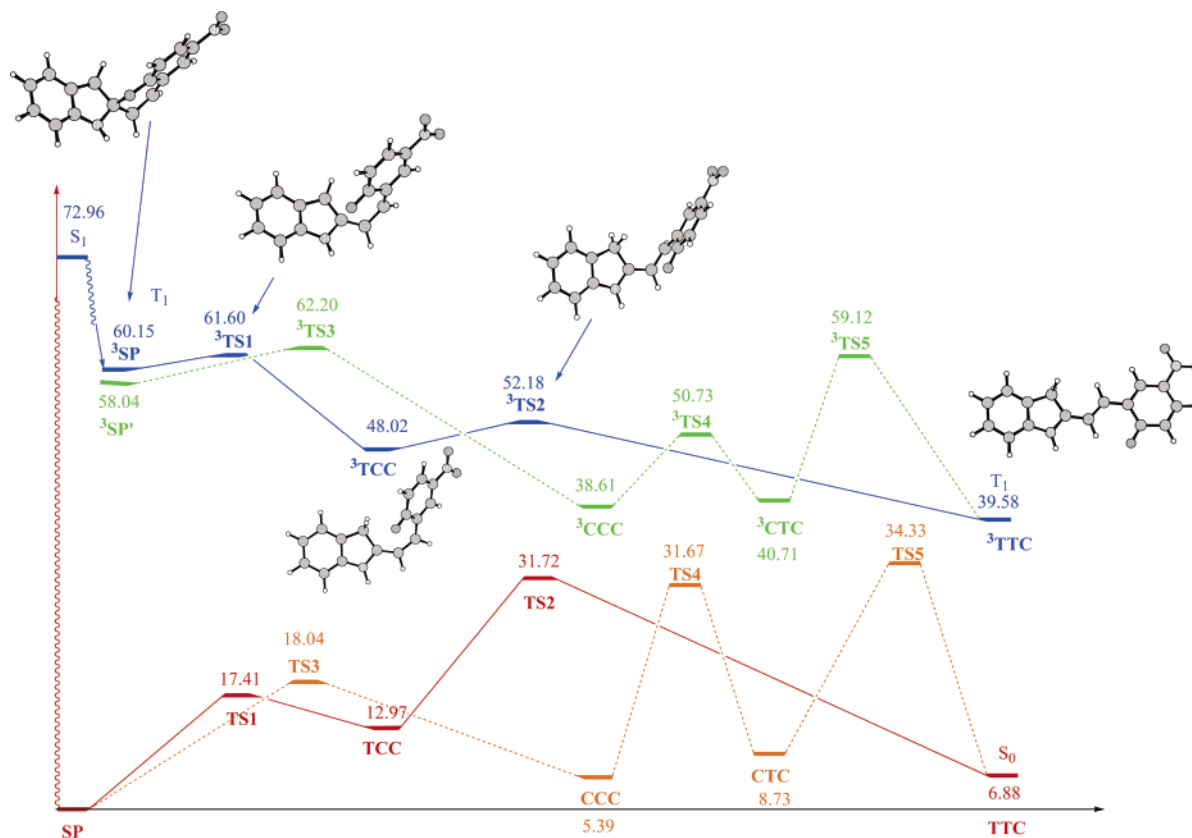


Figure 3. Triplet potential surface of coloration and decoloration of spiropyran (**SP-2**). Pathway A is in blue and pathway B in green. For comparison, the ground-state potential surfaces of coloration and decoloration of **SP-2** (in red and brown) are also illustrated.

TABLE 3: B3LYP/6-31G(d) Calculated Activation Energies for the Ring Opening Step and the *cis*–*trans* Isomerization on the Triplet (T_1) PES

code	X	Y	SP \rightarrow MC coloration		MC \rightarrow SP Decoloration		ΔE^+ decoloration – ΔE^+ coloration
			ΔE^+ ring opening	ΔE^+ <i>cis</i> – <i>trans</i>	ΔE^+ <i>trans</i> – <i>cis</i>	ΔE^+ ring–closure	
SP-1	H	H	0.82	8.34	16.45	16.16	8.11
SP-2	H	NO ₂	1.44	4.16	12.60	13.58	9.42
SP-3	Me	NO ₂	0.75	3.35	12.06	14.31	13.56
SP-4	H	MeO	2.62	14.25	22.42	12.74	8.17

decay via an intersystem crossing (ISC) to the triplet state. The coloration then proceeds to the T_1 state. In this section, we will discuss the reaction mechanisms of the SP–MC conversion on the triplet-state potential surface. We used **SP-2** ($X = \text{H}$, $Y = \text{NO}_2$) as a model compound to study the possible SP–MC conversion mechanisms on the triplet-state potential surface. The conversions between the closed form and open form of spiropyrans **SP-1** and **SP-4** were also investigated to address the substituent effect.

Similarly to the ground state, two reaction pathways of the SP–MC conversion on the triplet-state PES were found, that is, pathways A and B. The activation energies of the coloration on pathways A and B are 4.16 and 12.12 kcal/mol, respectively. The decoloration activation energies for pathways A and B are equal to 13.58 and 23.59 kcal/mol, respectively. The activation energies on pathway A for both coloration and decoloration, are much lower than those on pathway B. Therefore, we conclude that neither coloration nor decoloration prefers to proceed via pathway B. In the following we will only discuss pathway A on the triplet-state potential surface.

The relative energy of the relaxed triplet-state ^3SP with respect to its ground state is about 60.15 kcal/mol. The C–O cleavage transition state ($^3\text{TS1}$) is located and shown in Figure 3. The C_1 –O bond distance in $^3\text{TS1}$ is about 1.792 Å. It is much shorter than that in **TS1** (2.358 Å). The activation energy

for C–O cleavage on the triplet-state PES (1.44 kcal/mol) is much smaller than on the ground-state PES. The second step of coloration on the triplet-state PES (T_1) is *cis*–*trans* isomerization. The activation energy is calculated to be 4.16 kcal/mol.

The substituent effect on SP–MC conversion on the triplet potential surface was also investigated, and the activation energies of the SP–MC conversion for the **SP-1**, **SP-2**, **SP-3**, and **SP-4** are summarized in Table 3. In Table 3 the *cis*–*trans* isomerization is the rate-determining step for the coloration for all of these four species. Acceptor–acceptor pairs increase the activation energy, while donor–acceptor pairs lower the activation energy. For instance, the activation energy for **SP-2** ($X = \text{H}$, $Y = \text{NO}_2$) is 4.16 kcal/mol, while the activation energy drops slightly to 3.35 kcal/mol for the stronger donor–acceptor substituted spiropyran **SP-3** ($X = \text{Me}$, $Y = \text{NO}_2$). To the contrary, the coloration activation energy increases significantly to 14.25 kcal/mol for **SP-4** ($X = \text{H}$, $Y = \text{MeO}$).

As for the decoloration, the rate-determining step changes with different donor and acceptor combinations. For unsubstituted spiropyran (**SP-1**) and acceptor–donor substituted spiropyran (**SP-4** $X = \text{H}$, $Y = \text{MeO}$), the *trans*–*cis* isomerization is the rate-determining step. For the donor–acceptor substituted spiropyrans (**SP-2** $X = \text{H}$, $Y = \text{NO}_2$ and **SP-3** $X = \text{Me}$, $Y = \text{NO}_2$), ring closure becomes the rate-determining step.

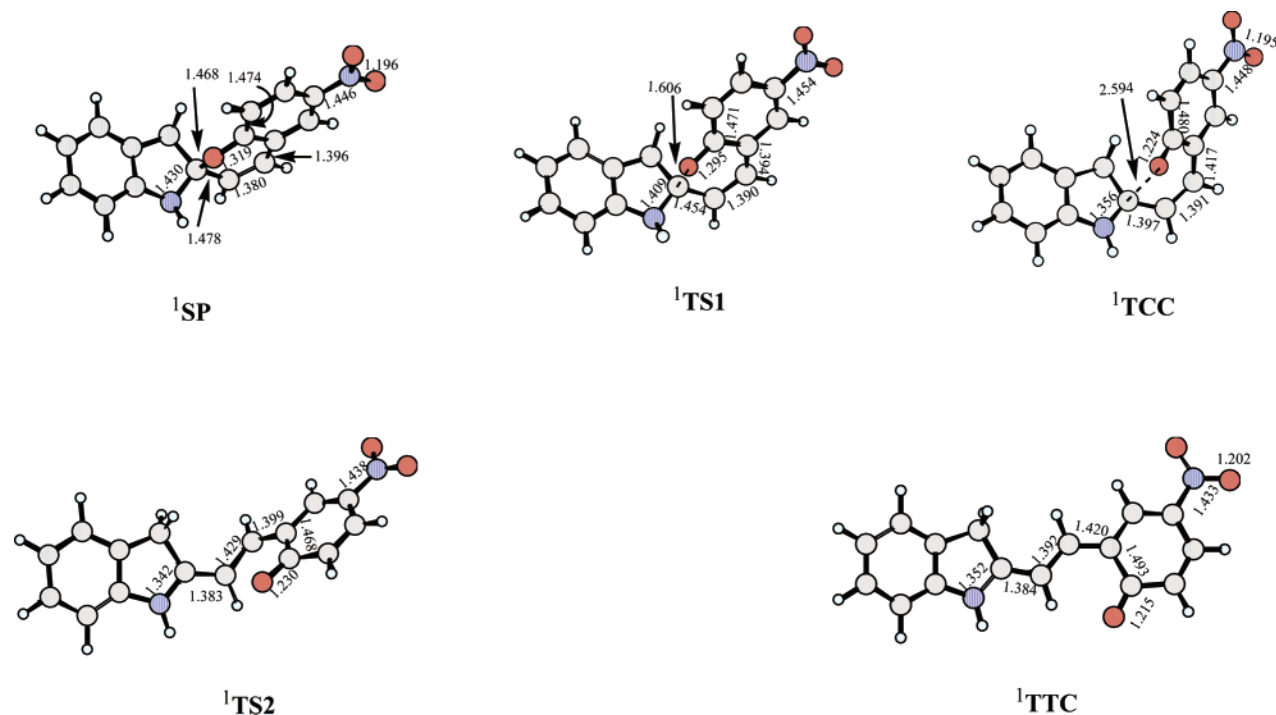


Figure 4. CIS/6-31G(d) optimized stationary points on the lowest excited singlet-state potential surface. The distances are in angstroms.

TABLE 4: TD-DFT Calculated Activation Energies of Coloration and Decoloration of Selected Four Spiroyrans on the Lowest Excited Singlet-State (S_1) PES

code	X	Y	coloration		decoloration		$\Delta E_{\text{decoloration}}^+ - \Delta E_{\text{coloration}}^+$
			$\Delta E_{\text{ring opening}}^+$	$\Delta E_{\text{cis-trans}}^+$	$\Delta E_{\text{trans-cis}}^+$	$\Delta E_{\text{ring-closure}}^+$	
SP-1	H	H	-0.22	11.27	2.80	33.24	21.97
SP-2	H	NO ₂	5.94	7.63	4.39	28.69	21.06
SP-3	Me	NO ₂	7.69	5.78	2.81	26.52	18.83
SP-4	H	MeO	-2.32	11.60	3.91	30.93	19.33

Unlike the ground state, in which spiroyrans with large BLA slightly favor decoloration ($\Delta E_{\text{decoloration}}^+ - \Delta E_{\text{coloration}}^+ < 0$), all substituent patterns favor coloration on the triplet-state PES (the $\Delta E_{\text{decoloration}}^+ - \Delta E_{\text{coloration}}^+$ values on the triplet-state PES for the considered species are positive), indicating a greater preference for coloration over decoloration.

III-F. Conversion between Spiroyrans and Merocyanines on the Lowest Excited Singlet-State Potential Surface. In this section we will discuss the reaction mechanism of SP-MC conversion on the lowest excited singlet-state PES. Only one pathway (pathway A) has been found. We have been unable to locate the transition state for the C–O cleavage on pathway B. Therefore, only reaction mechanisms on pathway A will be discussed. The CIS optimized stationary points on the S_1 potential energy surface for **SP-2** (X = H, Y = NO₂) are shown in Figure 4.

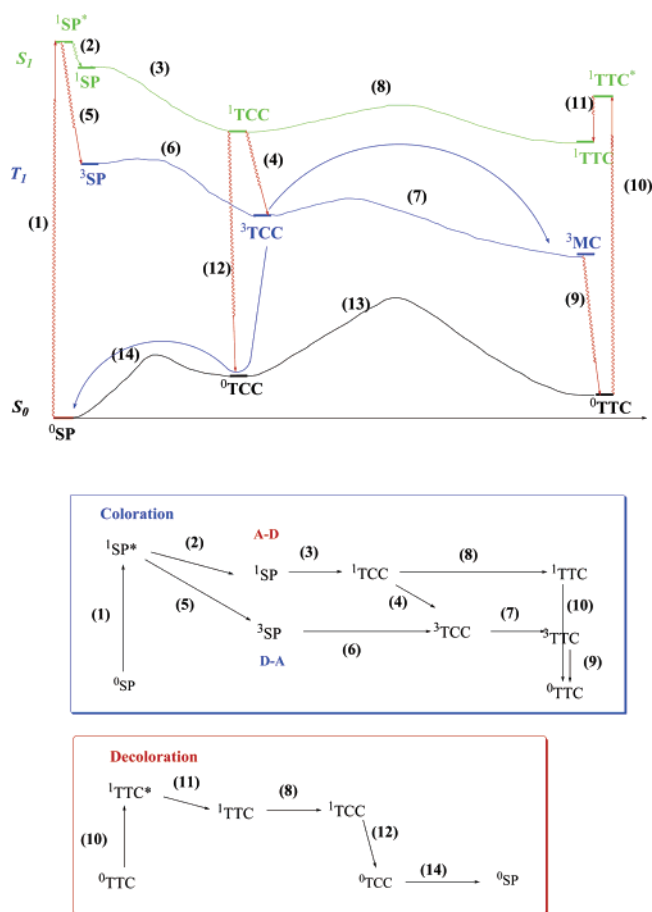
The C–O cleavage transition state (**¹TS1**) is an early transition state. The C₁–O distance (1.606 Å) is much shorter than **³TS1** and **TS1**, indicating that the C–O bond is far from being broken. Compared to **TS2** and **³TS2**, the *cis*–*trans* isomerization transition state **¹TS2** is a late transition state. The dihedral angle C₁–C₂–C₃–C₄ is about 120°, which is larger than those in the **TS2** and **³TS2** transition structures (~90°). Similarly, the substituent effects for the S_1 state were also investigated using model compounds **SP-1**, **SP-3**, and **SP-4**. The geometrical features of the optimized structures are found to be similar to each other. For instance, the optimized C–O cleavage transition states are all the earlier TSs with the C–O bond lengths being around 1.6 Å.

The TD-DFT calculated activation energies for the selected four spiroyrans are listed in Table 4. For unsubstituted and acceptor–donor substituted spiroyrans (**SP-1**, **SP-4**), the C–O cleavage activation energies are comparably negligible. The *cis*–*trans* isomerization is the rate-determining step, and its activation energy decreases as the BLA decreases. For donor–acceptor substituted spiroyrans, the *cis*–*trans* isomerization activation energy decreases as the BLA becomes smaller; however, the C–O cleavage activation energy increases and becomes the rate-determining step in **SP-4**. We expect that the C–O cleavage activation energy will further increase for stronger donor–acceptor pairs or more polar solvents.

For decoloration, the activation energies for the *trans*–*cis* isomerization are much smaller than the activation energies for the C–O bond formation (see Table 4). The ring closure step is the rate-determining step; its activation energy decreases as the BLA becomes smaller. The values of $\Delta E_{\text{decoloration}}^+ - \Delta E_{\text{coloration}}^+$ on the S_1 PES for **SP-1**, **SP-2**, **SP-3**, and **SP-4** are 22.0, 21.1, 18.8, and 19.3 kcal/mol, respectively. This indicates the greater preference of coloration over decoloration on the excited singlet-state PES.

III-G. Mechanistic Considerations of Photochemical Conversions between Spiropyran and Merocyanine. So far, we have investigated the coloration and decoloration of spiroyrans on the ground-state (S_0), the triplet-state (T_1), and the lowest excited singlet-state (S_1) PESs even though the efficiency of the intersystem crossing is still unknown for spiroyrans. Currently, all the conical intersection crossing points⁵³ between the S_0 , T_1 , and S_1 potential energy surfaces are being investigated

SCHEME 3



and the results of this study will be published elsewhere. However, even a simplified study that includes a comparison of the activation energies on the S_0 , T_1 , and S_1 PESs may provide useful information and help to better understand the photochemistry of SP-MC conversion. In Scheme 3, the three potential energy surfaces are charted together. A complete evolution of the photochemistry will be discussed below.

After the photoexcitation of the closed-form spiropyran, the conversion between the closed and open forms of spiropyrans may proceed on the excited singlet-state PES. The excited-state closed-form spiropyrans may also decay to the triplet state via the intersystem crossing, and then the C–O cleavage may proceed to the triplet state. Whether the reaction takes place on the singlet or triplet-state PES can be addressed in terms of the values of the activation energies for each state. Table 5 shows the activation energies for each step of the coloration and decoloration on the S_0 , T_1 , and S_1 PESs for the four selected spiropyrans.

By comparing the activation energies for the C–O cleavage step on the S_0 , T_1 , and S_1 PESs, one concludes that the C–O cleavage activation energy of the acceptor–donor substituted spiropyran (**SP-4**, $X = H$, $Y = \text{MeO}$) on the S_0 potential energy surface is much larger than those on the S_1 and T_1 PESs. This result rules out the possibility of C–O cleavage at the ground state. The C–O cleavage activation energy on the T_1 PES is calculated to be about 2.62 kcal/mol. The TD-DFT level energy for the CIS/6-31G(d) optimized transition structure is lower than for the **SP-4** closed form by 2.32 kcal/mol. In addition, TD-DFT single-point calculations using the CIS/6-31G(d) partially optimized structures (C–O fixed at distances varied from 1.5 to 1.8 Å, see Figure S1 of the Supporting Information) indicates that the C–O cleavage of **SP-4** on the S_1 PES is barrierless.

TABLE 5: Ground-State and Triplet-State Activation Energies for Coloration and Decoloration of Spiropyrans at the B3LYP/6-31G(d) Level and the TD-DFT Calculated Activation Energies for the Excited Singlet State Using the CIS Optimized Excited Singlet State Geometries

code	X–Y	S_0	T_1	$S_1(\text{TD-DFT})$
coloration				
C–O cleavage		$\Delta E_{\text{C–O cleavage}}^{\ddagger}$		
SP-1	H–H	21.61	0.82	−0.22
SP-2	H–NO ₂	17.41	1.44	5.94
SP-3	Me–NO ₂	15.44	0.75	7.69
SP-4	H–MeO	21.81	2.62	−2.32
<i>cis</i> – <i>trans</i> isomerization		$\Delta E_{\text{cis–trans}}^{\ddagger}$		
SP-1	H–H	14.77	8.34	11.27
SP-2	H–NO ₂	18.75	4.16	7.63
SP-3	Me–NO ₂	18.57	3.35	5.78
SP-4	H–MeO	13.08	14.25	11.60
decoloration				
<i>trans</i> – <i>cis</i> isomerization		$\Delta E_{\text{trans–cis}}^{\ddagger}$		
SP-1	H–H	20.45	16.45	2.80
SP-2	H–NO ₂	24.84	12.60	4.39
SP-3	Me–NO ₂	25.10	12.06	2.81
SP-4	H–MeO	18.93	22.42	3.91
ring closure		$\Delta E_{\text{cis–closed}}^{\ddagger}$		
SP-1	H–H	6.23	16.16	33.24
SP-2	H–NO ₂	4.44	13.58	28.69
SP-3	Me–NO ₂	3.32	14.31	26.52
SP-4	H–MeO	7.35	12.74	30.93

This suggests that the C–O cleavage should take place simultaneously as the species is excited to the excited singlet state. The activation energy for the second step (*cis*–*trans* isomerization) for **SP-4** on the S_1 PES is lower than on the S_0 and T_1 PESs by about 1.5 and 2.7 kcal/mol, respectively. Therefore, the *cis*–*trans* transformation for **SP-4** proceeds via the excited singlet state.

However, in the case of unsubstituted spiropyran **SP-1** ($X = Y = H$), the C–O cleavage activation energies on the T_1 PES are so small that C–O cleavage on the triplet-state surface cannot be ruled out. Nevertheless, the activation energy for the *cis*–*trans* isomerization on the T_1 PES becomes lower than on the S_1 surface; therefore, the *cis*–*trans* transformation proceeds more easily through the triplet state.

As the strengths of the donor–acceptor pairs increase (**SP-2**, **SP-3**), the activation energies on the T_1 PES for both the C–O cleavage and the *cis*–*trans* isomerization became lower than on the S_1 PES. We conclude that the coloration of the donor–acceptor substituted spiropyrans proceeds via the triplet state and involves formation of a triplet-state *trans*-merocyanine that decays to its ground state.

In brief, the colorations of unsubstituted and acceptor–donor substituted spiropyrans take place via either the excited singlet state or triplet state, while for the strong donor–acceptor substituted spiropyrans, coloration takes place only via the triplet state. This is also supported by the experimental observations that the substitution of the oxazine or pyran fragment of spirooxazines and spiropyrans with electron withdrawing groups favors the triplet manifold and leads to higher quantum yields of the conversion.^{14a,54}

The obtained results indicate that the process of photodecoloration of spiropyrans is relatively simpler. Only one reaction mechanism is found, regardless of the type of substituent patterns used (see Scheme 3). The open form of spiropyran ^0TTC is first promoted to its vertical state $^1\text{TCC}^*$ (**10**) and then relaxes to its excited state ^1TCC (**11**). The *trans*–*cis* transformation proceeds on the S_1 PES since the activation energies on the S_1 state PES are lower than those on the triplet-state and the ground-state PESs (**8**). The ring closure proceeds

on the ground-state PES after the S_1 state *cis*-intermediate decays to the ground state (**12**→**14**).

It is important to notice in Table 5 that, for the unsubstituted and acceptor–donor substituted spiropyrans (**SP-1**, **SP-4**), the activation energy required for the *cis*-intermediate to form the open *trans*-merocyanines on the triplet-state PES ($\Delta E^{\ddagger}_{\text{cis} \rightarrow \text{trans}(T_1)}$) is larger than the activation energy ($\Delta E^{\ddagger}_{\text{cis} \rightarrow \text{closed}(S_0)}$) required for the *cis*-intermediate to revert back to the closed-form spiropyrans, assuming that the decay of *cis*-merocyanines from the triplet state to its ground state is efficient. For instance, the values of $\Delta E^{\ddagger}_{\text{cis} \rightarrow \text{closed}(S_0)}$ on the ground state PES and $\Delta E^{\ddagger}_{\text{cis} \rightarrow \text{trans}(T_1)}$ on the triplet-state PES for **SP-4** ($X = \text{H}$, $Y = \text{MeO}$) are 7.35 and 14.25 kcal/mol, respectively. This means that the *cis*-form intermediate of **SP-2** and **SP-4** can revert back to the closed-form spiropyrans with a very high rate and thus produce no closed-form spiropyrans. However, for donor–acceptor substituted spiropyrans (**SP-1**, **SP-3**), the values of $\Delta E^{\ddagger}_{\text{cis} \rightarrow \text{trans}(T_1)}$ and $\Delta E^{\ddagger}_{\text{cis} \rightarrow \text{closed}(S_0)}$ are close to each other and thus enhance the transformation from the *cis*- to the *trans*-merocyanines. We expect that, with stronger donor–acceptor pairs or by increasing the polarity of the solvents, the values of $\Delta E^{\ddagger}_{\text{cis} \rightarrow \text{trans}(T_1)}$ can be tuned to be even smaller than $\Delta E^{\ddagger}_{\text{cis} \rightarrow \text{closed}(S_0)}$, and the *cis*–*trans* isomerization on the triplet-state PES would become the major reaction. This is the reason that 1',3',3'-trimethylspiro[2H-1-benzopyran-2,2'-indoline] (BIPS) has no practical value with respect to photochromism.⁵⁵ This is because unsubstituted BIPS has a very high rate of reverting back to closed-form spiropyrans, while a nitro group in the 6-position of benzopyran enhances photochromic activity toward the coloration.⁵⁶

IV. Conclusions

The reaction mechanisms of conversions between the closed-form and open-form spiropyrans (*trans*-merocyanine) on the ground-state (S_0), the triplet-state (T_1), and the first excited singlet-state (S_1) PESs have been investigated by nonempirical theoretical calculations. According to obtained results, we draw the following conclusions.

(1) There are two reaction pathways for the thermal conversions (coloration and decoloration) between the closed form and open form of spiropyrans (pathways A and B). Pathway A leads to the formation of TTC merocyanine, while pathway B results in the CTC isomer. Both pathways could be responsible for the coloration and decoloration of spiropyrans.

(2) The substituent effect on the SP-MC conversion on the ground-state PES has been investigated using a series of donor–acceptor substituted spiropyrans. The geometrical parameter BLA was used to correlate the strengths of the donor–acceptor pairs and the activation energies of coloration and decoloration. No simple relationship between the activation energy and the BLA is found. For the decoloration of spiropyrans on the ground-state PES, the *trans*–*cis* isomerization is always the rate-determining step. A monotonic relationship between the *trans*–*cis* isomerization barrier and the BLA values in *trans*-merocyanine is found. The solvent effect is similar to the substituent effect. Coloration is favored over decoloration when the polarities of the solvents increase.

(3) Similar to the ground state, two pathways (pathways A and B) of the SP-MC conversions of spiropyrans on the triplet-state PES have been studied. Both coloration and decoloration prefers to proceed via pathway A.

(4) The coloration and decoloration for substituted spiropyrans on the lowest excited singlet-state PES are two-step reactions. The rate-determining step changes when various substituents

are used. The values of $\Delta E^{\ddagger}_{\text{decoloration}}$ are much larger than the values of $\Delta E^{\ddagger}_{\text{coloration}}$, indicating the greater preference of coloration of spiropyrans over decoloration on the excited singlet-state PES.

(5) The data for computed potential energy surfaces for three states (S_1 , T_1 , and S_0) provides a comprehensive mechanistic view of the ultrafast photochemistry of spiropyrans. Whether the photocoloration of spiropyrans goes via the singlet state or triplet state crucially depends on the strengths of the substituents and the polarities of the solvents. The colorations of unsubstituted and acceptor–donor substituted spiropyrans take place via either the S_1 or the T_1 state, while for strong donor–acceptor substituted spiropyrans the coloration exclusively takes place on the triplet-state PES. Only one reaction mechanism is found for the photodecoloration of spiropyrans regardless of which kind of substituent is used. The unsubstituted and acceptor–donor substituted spiropyrans have a high rate of decoloration and therefore have no practical value with respect to photochromism. On the other hand, strong donor–acceptor pairs significantly enhance the photochromic activity of spiropyrans.

Acknowledgment. This work was facilitated in part by NSF Grant No. 9805465 & 9706268, NSF Grant No. CTS-0102680, ONR Grant No. N00014-98-1-0592, and the Army High Performance Computing Research Center under the auspices of the Department of the Army, Army Research Laboratory cooperative agreement number DAAH04-95-2-0003/contract number DAAH04-95-C-0008. We would like to thank the Mississippi Center for Supercomputing Research for a generous allotment of computer time. S.Y.H. thanks Dr. William K. Wymond and Dr. Yihan Shao for their helpful discussion.

Supporting Information Available: The B3LYP/g-31G(d) and CIS/6-31G(d) optimized XYZ coordinates and the calculated total energies of the closed-form and open-form spiropyran, transition states, and the intermediates involved in the conversion reaction between the closed- and open-form spiropyrans. Figures showing the CIS/6-31G(d) and TDDFT B3LYP/6-31G(d) calculated total energies of the CIS/6-31G(d) partially optimized structures. This material is available free of charge via the Internet at <http://pubs.acs.org>.

References and Notes

- (1) Bertelson, R. C., Photochromic Processes Involving Heterolytic Cleavage. In *Techniques of Chemistry*; Brown, G. H., Ed.; Wiley-Interscience: 1971; Vol. III, pp 45–433.
- (2) Duerr, H.; Bouas-Laurent, H. *Photochromism: Molecules and Systems*; Elsevier: New York, 1990.
- (3) Rouhi, A. M. *C&EN* **2000**, 40.
- (4) Willner, I.; Katz, E.; Willner, B.; Blonder, R.; Heleg-Shabtai, V.; Buckman, A. F. *Biosens. Bioelectron.* **1997**, 12, 337.
- (5) (a) Willner, I. *Acc. Chem. Res.* **1997**, 30, 347. (b) Willner, I.; Rubin, S.; Shatzmiller, R.; Zor, T. *J. Am. Chem. Soc.* **1993**, 115, 8690. (c) Garcia, A. A.; Cherian, S.; Park, J.; Gust, D.; Jahnke, F.; Rosario, R. *J. Phys. Chem.* **2000**, 104, 103.
- (6) (a) Gugliemetti, R. In *Photochromism-Molecules and Systems, Studies in Organic Chemistry*, 40; Durr, H., Bouas-Laurent, H., Eds.; Elsevier: Amsterdam, 1990; p 314, p 493, p 879. (b) *Organic Photochromic and Thermochromic Compounds*, Crano, J. C., Gugliemetti, R., Eds.; Plenum Press: New York, Vol. 1 and 2, 1999.
- (7) Becker, R. S.; Michl, J. *J. Am. Chem. Soc.* **1996**, 88, 5931.
- (8) Berkovic, G.; Krongauz, V.; Weiss, V. *Chem. Rev.* **2000**, 100, 1741.
- (9) (a) Salemi-Delvaux, C.; Luccioni-Houze, B.; Baillet, G.; Giusti, G.; Gugliemetti, R. *J. Photochem. Photobiol., A* **1995**, 91, 223. (b) Pimienta, V.; Lavabre, D.; Levy, G.; Samat, A.; Gugliemetti, R.; Mischeau, J. C. *J. Phys. Chem.* **1996**, 100, 4485.
- (10) Tamai, N.; Miyasaka, H. *Chem. Rev.* **2000**, 100, 1875.
- (11) Campredon, M.; Gugliemetti, R.; Samat, A.; Alberti, A. *J. Chem. Phys.* **1994**, 91, 1830.

- (12) (a) Görner, H.; Chibisov, A. K. *J. Chem. Soc., Faraday Trans.* **1998**, *94*, 2557. (b) Chibisov, A. K.; Görner, H. *Chem. Phys.* **1998**, *237*, 425.
- (13) Wojtyk, J. T.; Kazmaier, P. M.; Buncle, E. *Chem. Mater.* **2001**, *13*, 2547.
- (14) (a) Görner, H. *Chem. Phys. Lett.* **1998**, *282*, 381. (b) Görner, H. *Chem. Phys.* **1997**, *222*, 315. (c) Bohne, C.; Fan, M. G.; Li, Z. H.; Laing, Y. C.; Luszytyk, J.; Scaiano, J. C. *J. Photochem. Photobiol., A* **1992**, *66*, 79.
- (15) (a) Görner, H. *Chem. Phys. Lett.* **1998**, *282*, 381. (b) Bohne, C.; Fan, M. G.; Li, Z. H.; Liang, Y. C.; Luszytyk, J.; Scaiano, J. C. *J. Photochem. Photobiol., A* **1992**, *66*, 79.
- (16) Malatesta, A.; Neri, C.; Wis, M. L.; Montanari, L.; Millini, R. *J. Am. Chem. Soc.* **1997**, *119*, 3451.
- (17) (a) Görner, H.; Atabekyan, L. S.; Chibisov, A. K. *Chem. Phys. Lett.* **1996**, *260*, 59. (b) Salemi, C.; Giusti, G.; Guglielmetti, R. *J. Photochem. Photobiol., A* **1995**, *86*, 247. (c) Ricard, R.; Sauvage, P.; Wan, C. S. K.; Weedon, A. C.; Wong, D. F. *J. Phys. Chem.* **1986**, *90*, 62.
- (18) (a) Marfisi, C.; Verlaque, P.; Davidovics, G.; Pourcin, J.; Pizzala, L.; Aycard, J. P.; Bodot, H. *J. Phys. Chem.* **1983**, *87*, 5333. (b) Tamaki, T.; Sakuragi, M.; Ichimura, K.; Aori, K. *Chem. Phys. Lett.* **1989**, *161*, 23.
- (19) Day, P. N.; Wang, Z.; Patchter, R. *J. Phys. Chem.* **1995**, *99*, 9730.
- (20) Maurel, F.; Aubard, J.; Rajzmann, M.; Guglielmetti, R.; Samat, A. *J. Chem. Soc., Perkin Trans. 2* **2002**, 1307.
- (21) (a) Le Beuze, A.; Botrel, A.; Appriou, P.; Guglielmetti, R. *Tetrahedron* **1979**, *35*, 31. (b) Zerbetto, F.; Monti, S.; Orlandi, G. *J. Chem. Soc., Faraday Trans. 2* **1984**, *80*, 1513.
- (22) Celani, P.; Bernardi, F.; Olivucci, M.; Robb, M. A. *J. Am. Chem. Soc.* **1997**, *119*, 10815.
- (23) (a) Bauschlicher, C. W. *Chem. Phys. Lett.* **1995**, *246*, 40. (b) El-Azhary, A. A.; Suter, H. U. *J. Phys. Chem.* **1996**, *100*, 15056.
- (24) (a) Lee, C.; Yang, W.; Parr, R. *Phys. Rev. B* **1988**, *37*, 785. (b) Becke, A. D. *J. Chem. Phys.* **1993**, *98*, 5648. (c) Miehlisch, B.; Savin, A.; Stoll, H.; Preuss, H. *Chem. Phys. Lett.* **1989**, *90*, 5622. (d) Stephens, P. J.; Devlin, F. J.; Chabalowski, C. F.; Frisch, M. J. *J. Phys. Chem.* **1994**, *98*, 11623.
- (25) Schlegel, H. B. *J. Comput. Chem.* **1982**, *3*, 214.
- (26) Cancès, M. T.; Mennucci, V.; Tomasi, J. *J. Chem. Phys.* **1997**, *107*, 3032.
- (27) (a) Hariharan, P. C.; Pople, J. A. *Chem. Phys. Lett.* **1972**, *66*, 217. (b) Hehre, W. J.; Radom, L.; Schleyer, P. v. R.; Pople, J. A. *Ab Initio Molecular Orbital Theory*; Wiley: New York, 1986.
- (28) (a) Holmén, A.; Broo, A. *Int. J. Quantum Chem.* **1995**, *QBS22*, 113. (b) Broo, A.; Holmén, A. *Chem. Phys.* **1996**, *211*, 147.
- (29) (a) Roos, B. O. *Acc. Chem. Res.* **1999**, *32*, 137. (b) Davidson, E. R. *Chem. Rev.* **1991**, *91*, 649.
- (30) See, for example, Roos, B. O. In *Ab initio Methods in Quantum Chemistry II*, Lawley, K. P., Ed.; J. Wiley & Sons Ltd: New York, 1987; p 399.
- (31) Bauernschmitt, R.; Häser, M.; Treutler, O.; Ahlrichs, R. *Chem. Phys. Lett.* **1997**, *264*, 573.
- (32) Straman, R. E.; Scuseria, G. E.; Frisch, M. J. *J. Chem. Phys.* **1998**, *109*, 8218.
- (33) Van Caillie, C.; Amos, R. D. *Chem. Phys. Lett.* **2000**, *317*, 159.
- (34) Foresman, J. B.; Head-Gordon, M.; Pople, J. A.; Frisch, M. J. *J. Phys. Chem.* **1992**, *96*, 135.
- (35) (a) Parusel, A. B. J.; Rettig, W.; Sudholt, W. *J. Phys. Chem. A* **2002**, *106*, 804. (b) Sheng, Y.; Leszczynski, J. *Collect. Czech. Chem. Commun.* **2004**, *69*, 47.
- (36) Frisch, M. J.; Trucks, G. W.; Schlegel, H. B.; Scuseria, G. E.; Robb, M. A.; Cheeseman, J. R.; Zakrzewski, V. G.; Montgomery, J. A.; Stratmann, R. E., Jr.; Burant, J. C.; Dapprich, S.; Millam, J. M.; Daniels, A. D.; Kudin, K. N.; Strain, M. C.; Farkas, O.; Tomasi, J.; Barone, V.; Cossi, M.; Cammi, R.; Mennucci, B.; Pomelli, C.; Adamo, C.; Clifford, S.; Ochterski, J.; Petersson, G. A.; Ayala, P. Y.; Cui, Q.; Morokuma, K.; Malick, D. K.; Rabuck, A. D.; Raghavachari, K.; Foresman, J. B.; Cioslowski, J.; Ortiz, J. V.; Baboul, A. G.; Stefanov, B. B.; Liu, G.; Liashenko, A.; Piskorz, P.; Komaromi, I.; Gomperts, R.; Martin, R. L.; Fox, D. J.; Keith, T.; Al-Laham, M. A.; Peng, C. Y.; Nanayakkara, A.; Gonzalez, C.; Challacombe, M.; Gill, P. M. W.; Johnson, B. G.; Chen, W.; Wong, M. W.; Andres, C. L.; Head-Gordon, M.; Replogle, E. S.; Pople, J. A. *Gaussian 98*, Revision A.10; Gaussian, Inc., Pittsburgh, PA, 1998.
- (37) (a) Ernsting, N. P.; Arthen-Engeland, T. *J. Phys. Chem.* **1991**, *95*, 5502. (b) Nakatsu, K.; Yoshioka, H. *Kwansei Gakuin University Nat. Sci. Rev.* **1996**, *1*, 21.
- (38) Hobbey, J.; Malatesta, V. *Phys. Chem. Chem. Phys.* **2000**, *2*, 57.
- (39) (a) Aubard, J.; Maurel, F.; Buntinx, G.; Guglielmetti, R.; Lévi, G. *Mol. Cryst. Liq. Cryst.* **2000**, *345*, 203. (b) Delbaere, S.; Bochu, C.; Azaroual, N.; Buntinx, G.; Vermeersch, G. *J. Chem. Soc., Perkin Trans. 2* **1997**, 1499.
- (40) Futami, Y.; Chin, M. L. S.; Kudoh, S.; Takayanagi, M.; Nakata, M. *Chem. Phys. Lett.* **2003**, *370*, 460.
- (41) Cottone, G.; Noto, R.; Manna, G. L. *Chem. Phys. Lett.* **2004**, *388*, 218.
- (42) Bercovici, T.; Heiligman-Rim, R.; Fischer, E. *Mol. Photochem.* **1969**, *1*, 23.
- (43) (a) Aramaki, S.; Atkinson, G. H. *Chem. Phys. Lett.* **1990**, *170*, 181. (b) Buncel, E.; Kazmeier, P. M.; Keum, S. R. *Can. J. Chem.* **1991**, *69*, 1940.
- (44) (a) Gorman, C. B.; Marder, S. R. *Proc. Natl. Acad. Sci. U.S.A.* **1993**, *90*, 11297. (b) Sheng, Y.; Jiang, Y. *J. Chem. Soc., Faraday Trans.* **1998**, *94*, 1929.
- (45) Brooker, L. G. S.; Keyes, G. H.; Sprague, R. H.; Vandyke, R. H.; Vanlare, E.; Vanzandt, G.; White, F. L.; Cressman, H. W. J.; Dent, S. G. *J. Am. Chem. Soc.* **1951**, *73*, 5332.
- (46) (a) Meyers, F.; Marder, S. R.; Pierce, B. M.; Brédas, J. L. *J. Am. Chem. Soc.* **1994**, *116*, 10703. (b) Marder, S. R.; Gorman, C. B.; Meyers, F.; Perry, J. W.; Bourhill, G.; Brédas, J. L.; Pierce, B. M. *Science* **1994**, *265*, 632. (c) Sheng, Y.; Jiang, Y.; Wang, X.-C. *J. Chem. Soc., Faraday Trans.* **1998**, *94*, 47.
- (47) (a) Görner, H. *Phys. Chem. Chem. Phys.* **2001**, *3*, 416. (b) Sueishi, Y.; Ohcho, M.; Nishimura, N. *Bull. Chem. Soc. Jpn.* **1985**, *58*, 2608. (c) Levitus, M.; Talhavini, M.; Negri, R. M.; Atvars, T. D. Z.; Aramendia, P. F. *J. Phys. Chem.* **1997**, *101*, 7680. (d) Pfeifer-Fukumura, U. *J. Photochem. Photobiol., A* **1997**, *111*, 145.
- (48) Flannery, J. B., Jr. *J. Am. Chem. Soc.* **1968**, *90*, 5660.
- (49) Bercovici, T.; Heiligman-Rim, R.; Fischer, E. *Mol. Photochem.* **1969**, *1*, 23.
- (50) (a) Bercovici, T.; Heiligman, R.; Fischer, E. *Mol. Photochem.* **1969**, *1*, 23. (b) Bertelson, R. C. Photochromism. In *Techniques in Chemistry*; Brown, G. H., Ed.; Wiley-Interscience, New York, 1971; Vol. 3, p 45.
- (51) Kiesswetter, R.; Pustet, N.; Brandl, F.; Mannschreck, A. *Tetrahedron: Asymmetry* **1999**, *10*, 4677.
- (52) Kiesswetter, R.; Burgemeister, T.; Mannschreck, A. *Enantiomer* **1994**, *4*, 289.
- (53) (a) Bearpark, M. J.; Robb, M. A.; Schlegel, H. B. *Chem. Phys. Lett.* **1994**, *223*, 269. (b) Bernardi, F.; Olivucci, M.; Robb, M. A. *Chem. Soc. Rev.* **1996**, *25*, 321 and references therein.
- (54) (a) Chibisov, A. K.; Marevtsev, V. S.; Görner, H. *J. Photochem. Photobiol., A* **2003**, *159*, 233. (b) Chibisov, A. K.; Görner, H. *J. Phys. Chem. Photobiol., A* **1997**, *105*, 261. (c) Chibisov, A. K.; Görner, H. *J. Phys. Chem. A* **1997**, *101*, 4305. (d) Favaro, G.; Masetti, F.; Mazzucato, U.; Ottavi, G.; Allegrini, P.; Malatesta, V. *J. Chem. Soc., Faraday Trans.* **1994**, *90*, 333.
- (55) Bercovici, T.; Heiligman-Rim, R.; Fischer, E. *Mol. Photochem.* **1969**, *1*, 23.
- (56) (a) Aramaki, S.; Atkinson, G. H. *Chem. Phys. Lett.* **1990**, *170*, 181. (b) Buncel, E.; Kazmeier, P. M.; Keum, S. R. *Can. J. Chem.* **1991**, *69*, 1940.